Supplementary Information for

A Comparative Nanomechanical Study of Antibody and Nanobody Binding to SARS-CoV-2 Variants

Luis F. Cofas-Vargas[*a], Gustavo E. Olivos-Ramirez[a], Siewert J. Marrink[b] and Adolfo B. Poma[*a]

[a]*Biosystems and Soft Matter Division, Institute of Fundamental Technological Research, Polish Academy of Sciences, ul. Pawińskiego 5B, 02-106 Warsaw, Poland.*
[b]*Groningen Biomolecular Sciences and Biotechnology Institute, University of Groningen, Nijenborgh 7, 9747 AG Groningen, The Netherlands.*

* Corresponding authors

This file includes:

Supplementary Figures S1 to S19

Tables S1-S11

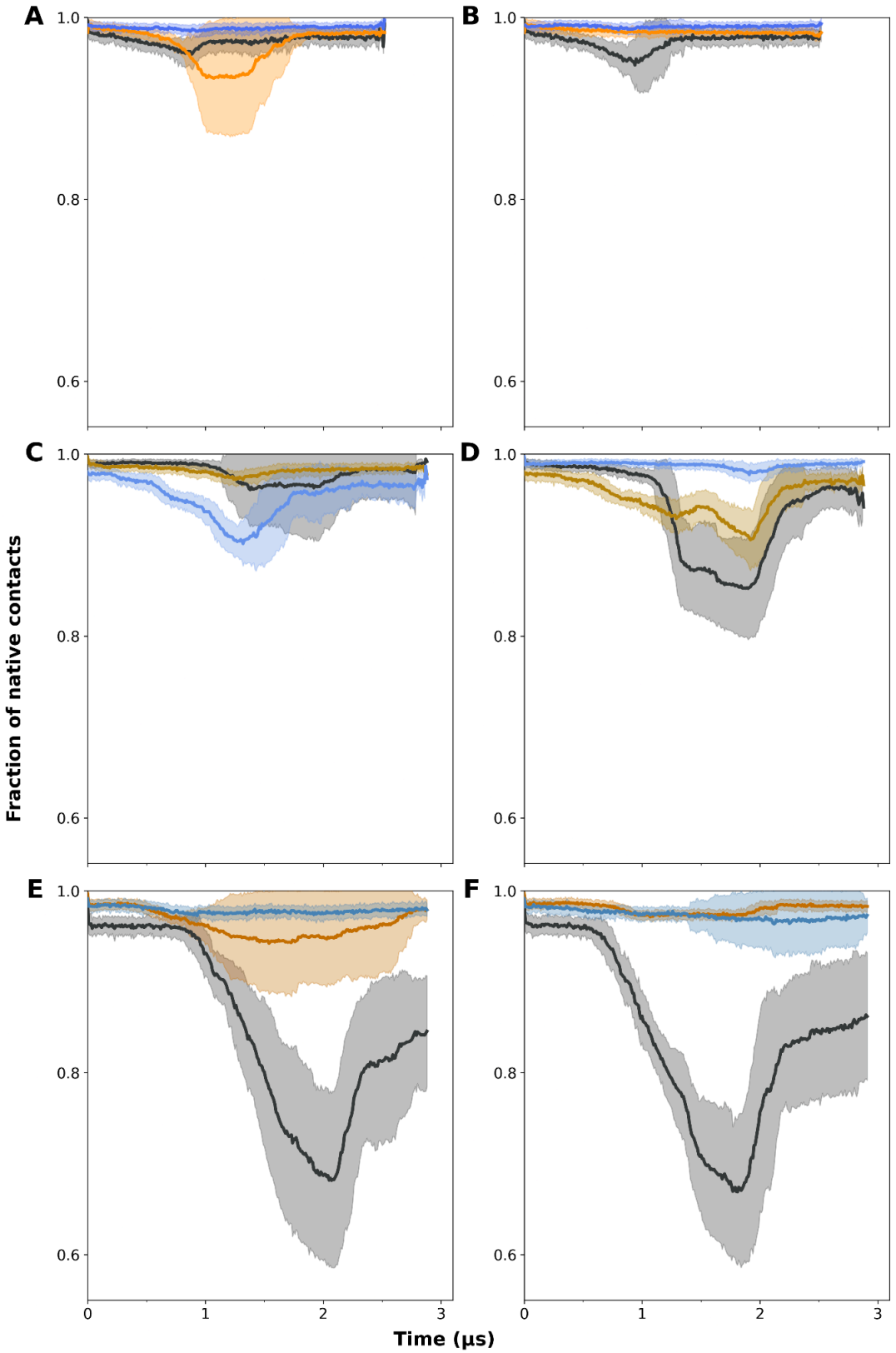

Figure S1. Contact frequency profiles over simulation time for RBD/Ab WT complexes. Timeline of the fraction of native contacts for the RBD and Ab H and L chains. RBD is shown in gray, H chains in orange/yellow, and L chains in blue. Panels in the left column (A, C, E) show SMD pulling from the H chain, and panels in the right column (B, D, F) show pulling from the L chain. Each row corresponds to a different complex: row 1, RBD/PDI-231 WT; row 2, S2XS259; row 3, R1-32.

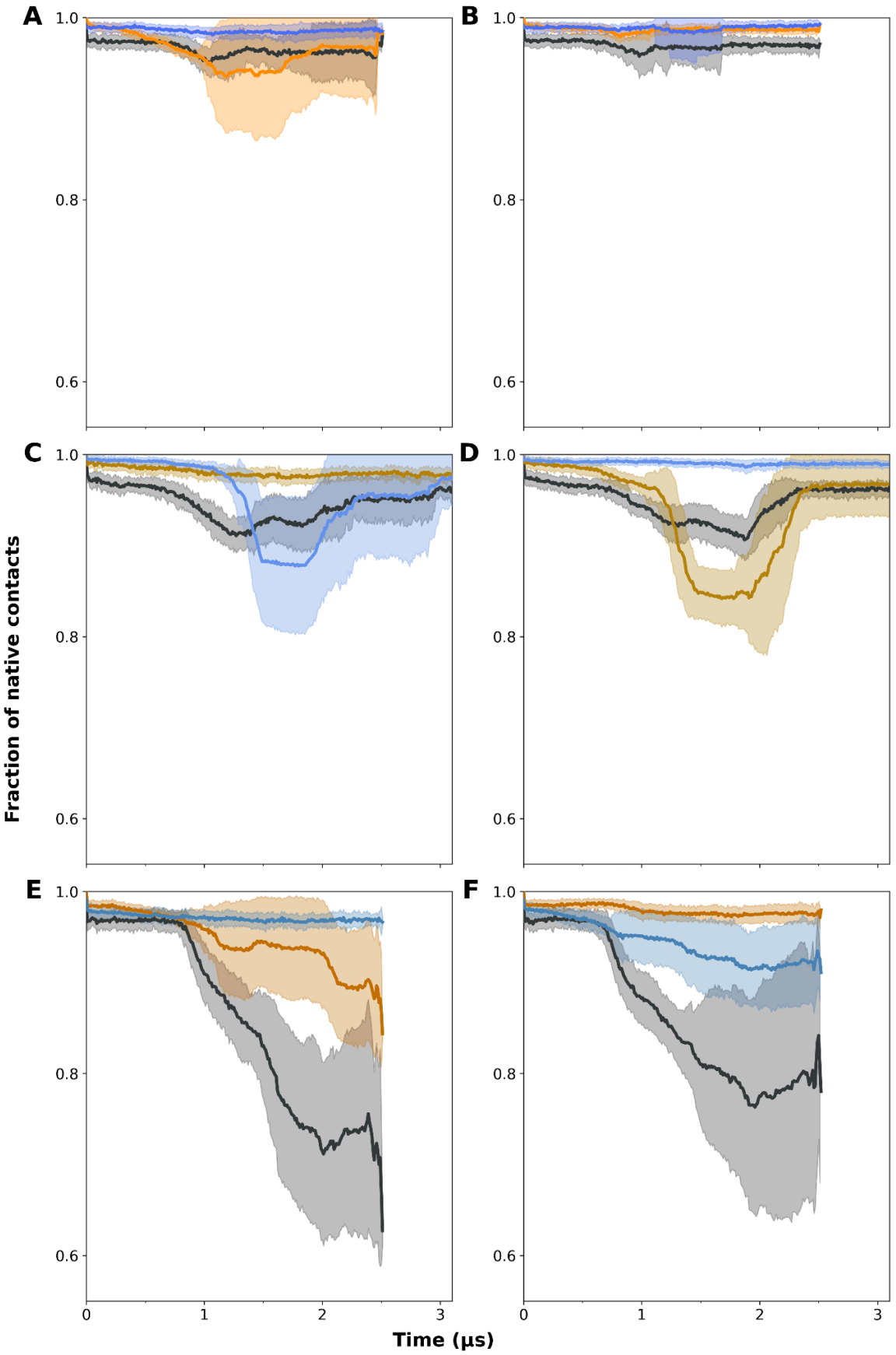

Figure S2. Contact frequency profiles over simulation time for RBD/Ab BA.4 complexes. Same as Figure S1.

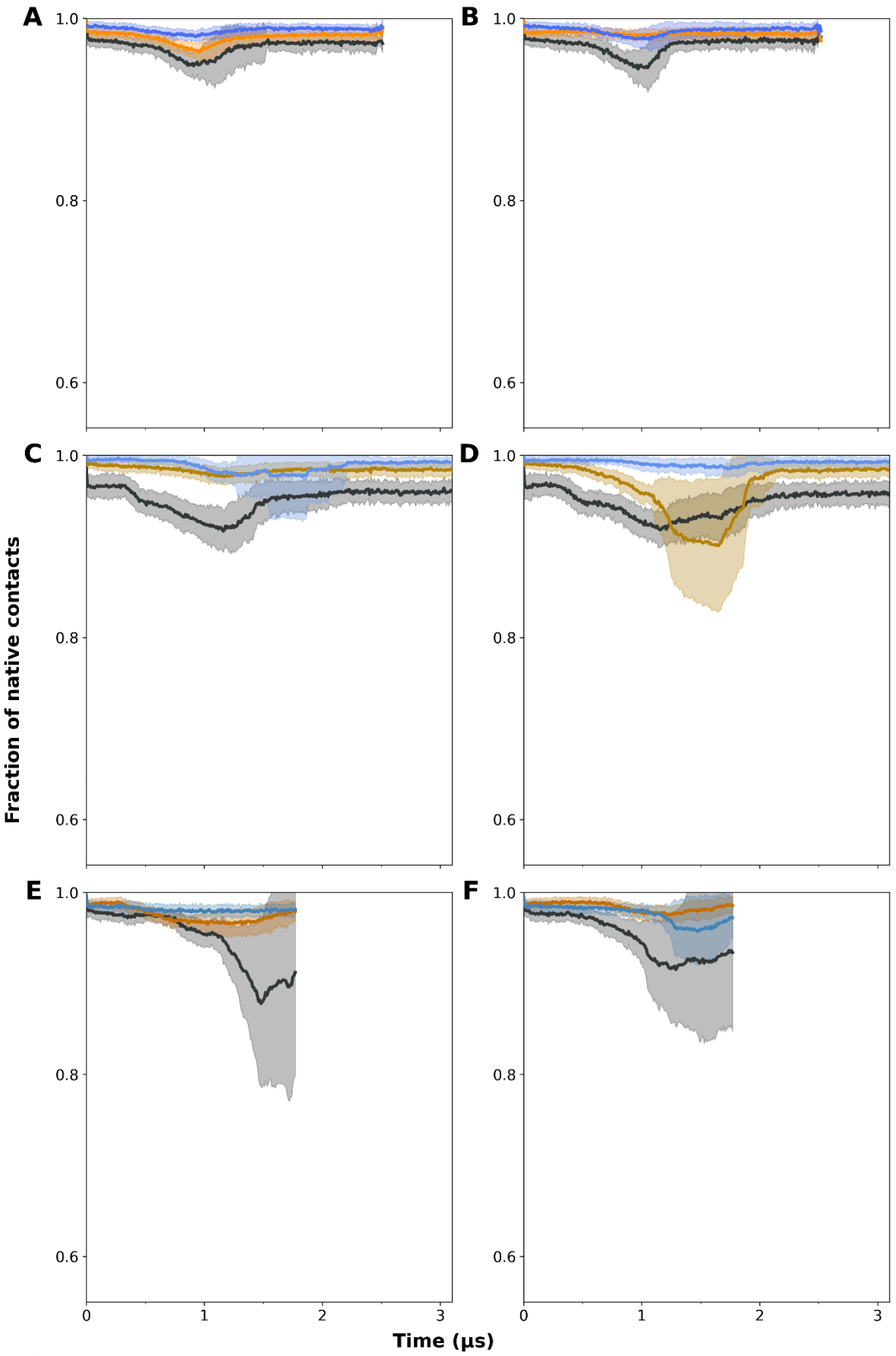

Figure S3. Contact frequency profiles over simulation time for RBD/Ab JN.1 complexes. Same as Figure S1

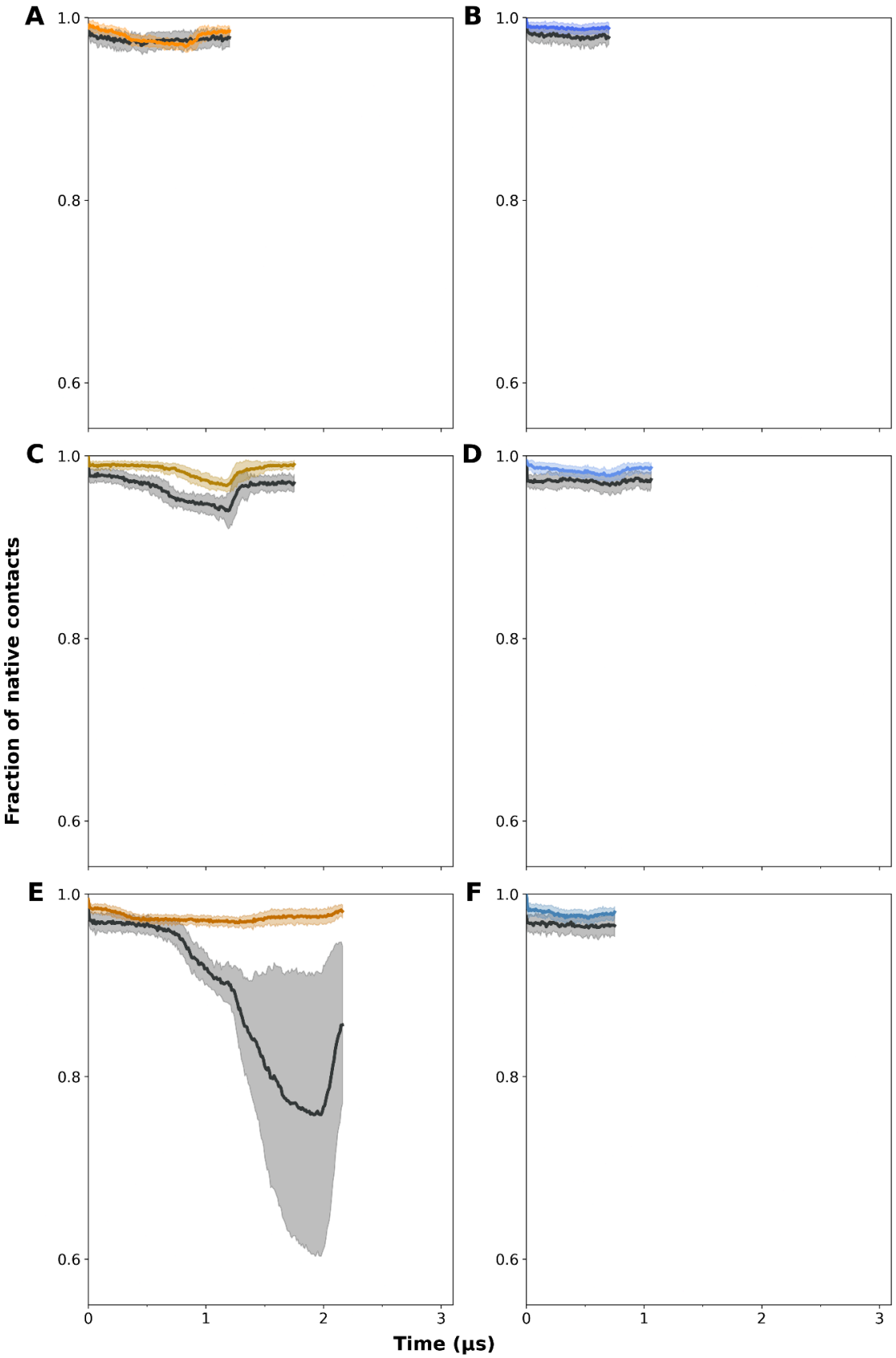

Figure S4. Mechanical response of Contact frequency profiles over simulation time for the Ab/RBD WT complexes under constant-velocity pulling from individual chains. Force-displacement profiles are shown of (A, B) PDI-231, (C, D) S2X259, and (E, F) R1-32. Pulling was applied from the H chain (left column) or the L chain (right column). Solid lines correspond to the mean response.

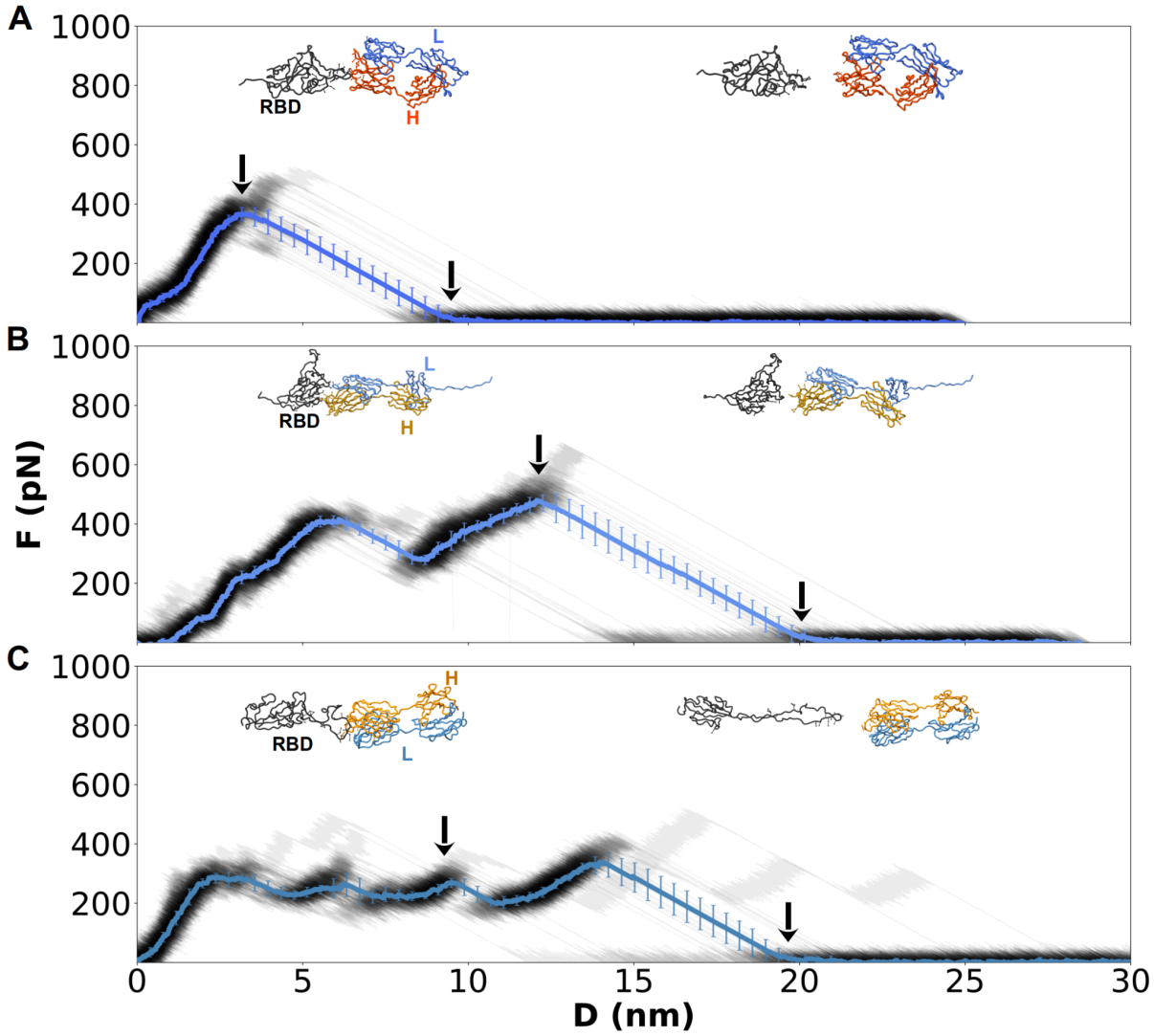

Figure S5. Mechanical response of Ab/RBD WT complexes under constant-velocity pulling from the L chain. Force–displacement profiles are shown for (A) PDI-231, (B) S2X259, and (C) R1-32 (gray traces, mean in color). Insets display representative structures at the maximum force (Fmax, left arrow) and after dissociation (right arrow). Error bars denote standard deviations across 50 independent trajectories.

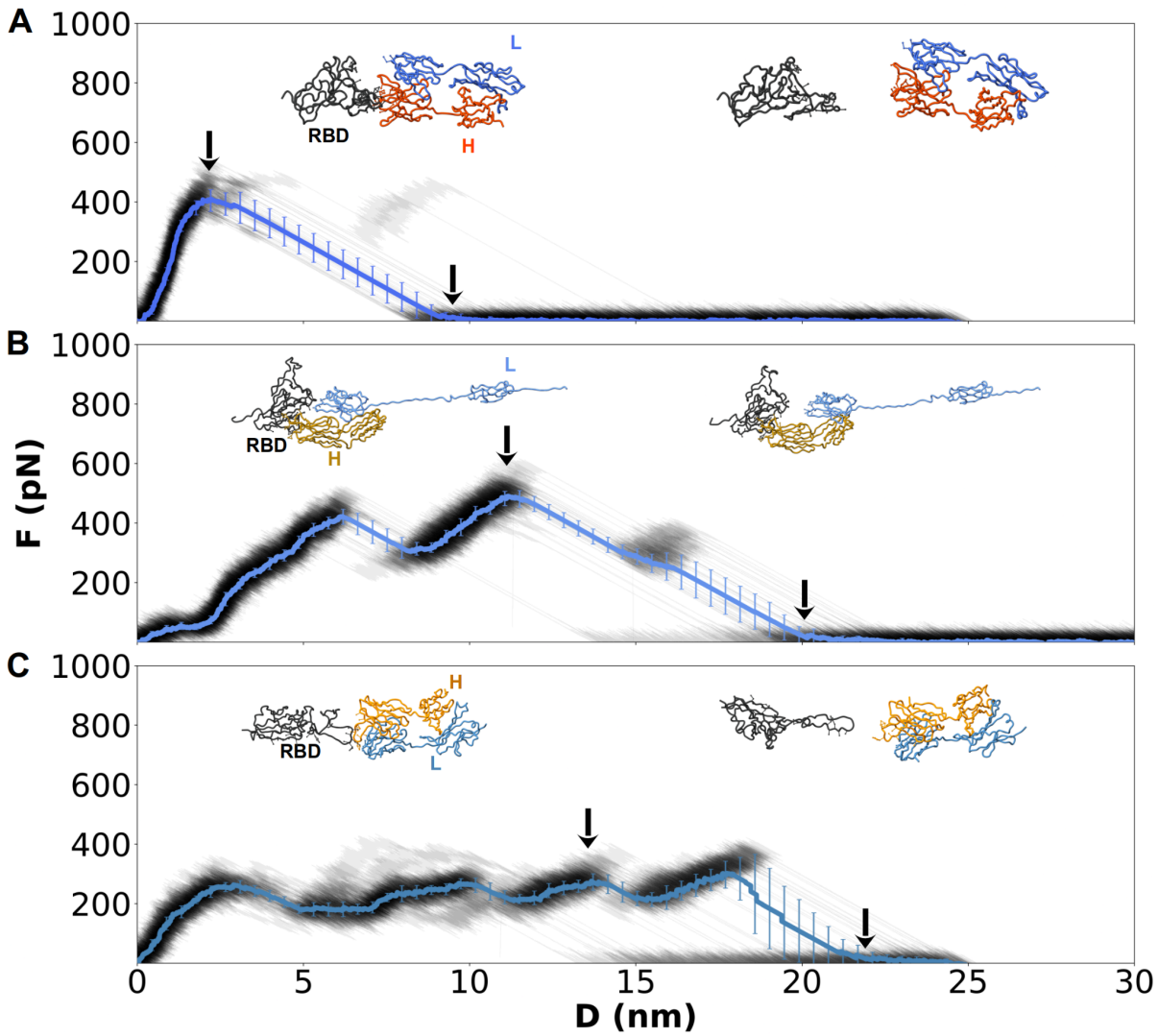

Figure S6. Mechanical response of Ab/RBD BA.4 complexes under constant-velocity pulling from the L chain. Same as Figure S4.

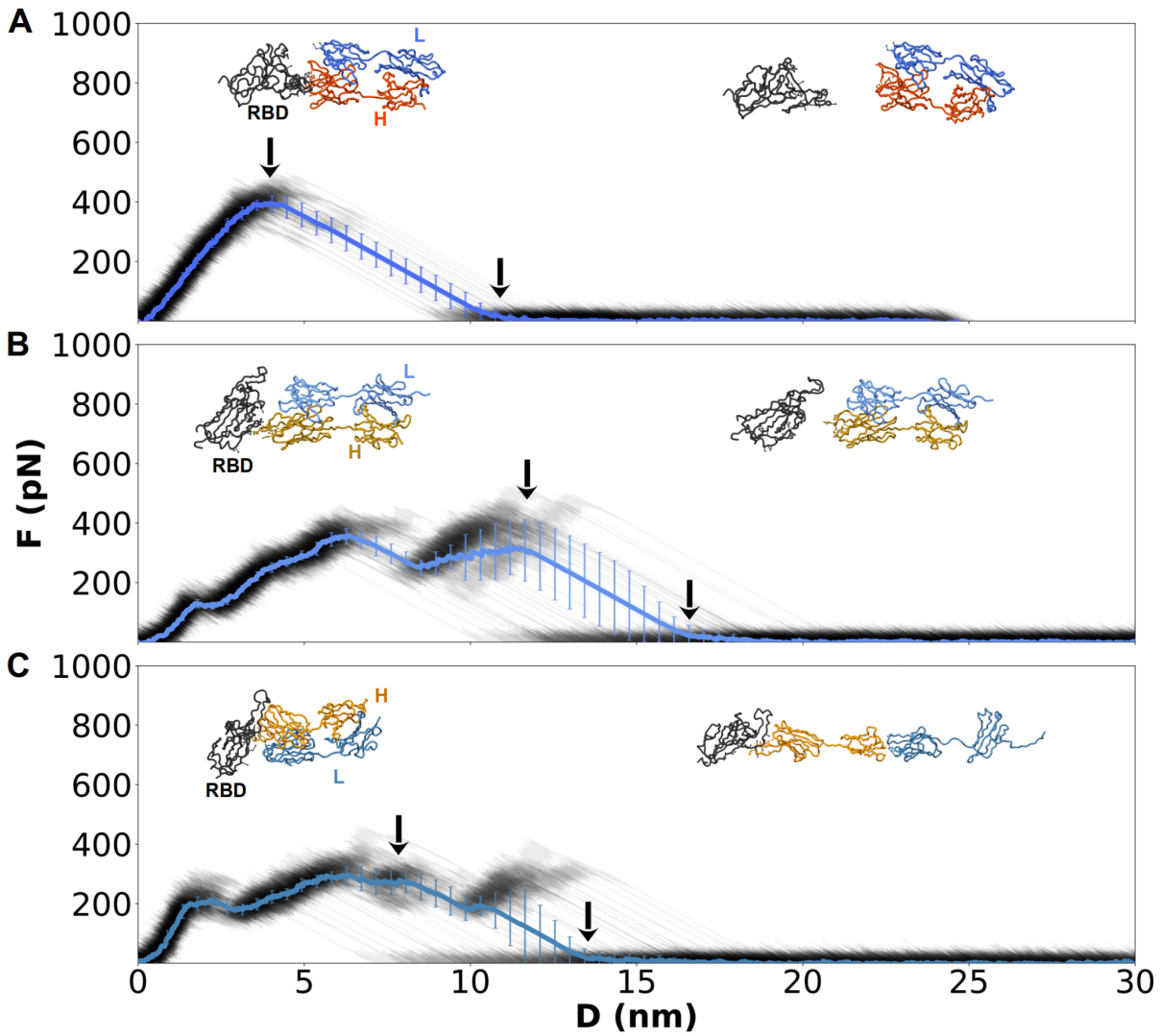

Figure S7. Mechanical response of Ab/RBD JN.1 complexes under constant-velocity pulling from the L chain. Same as Figure S4.

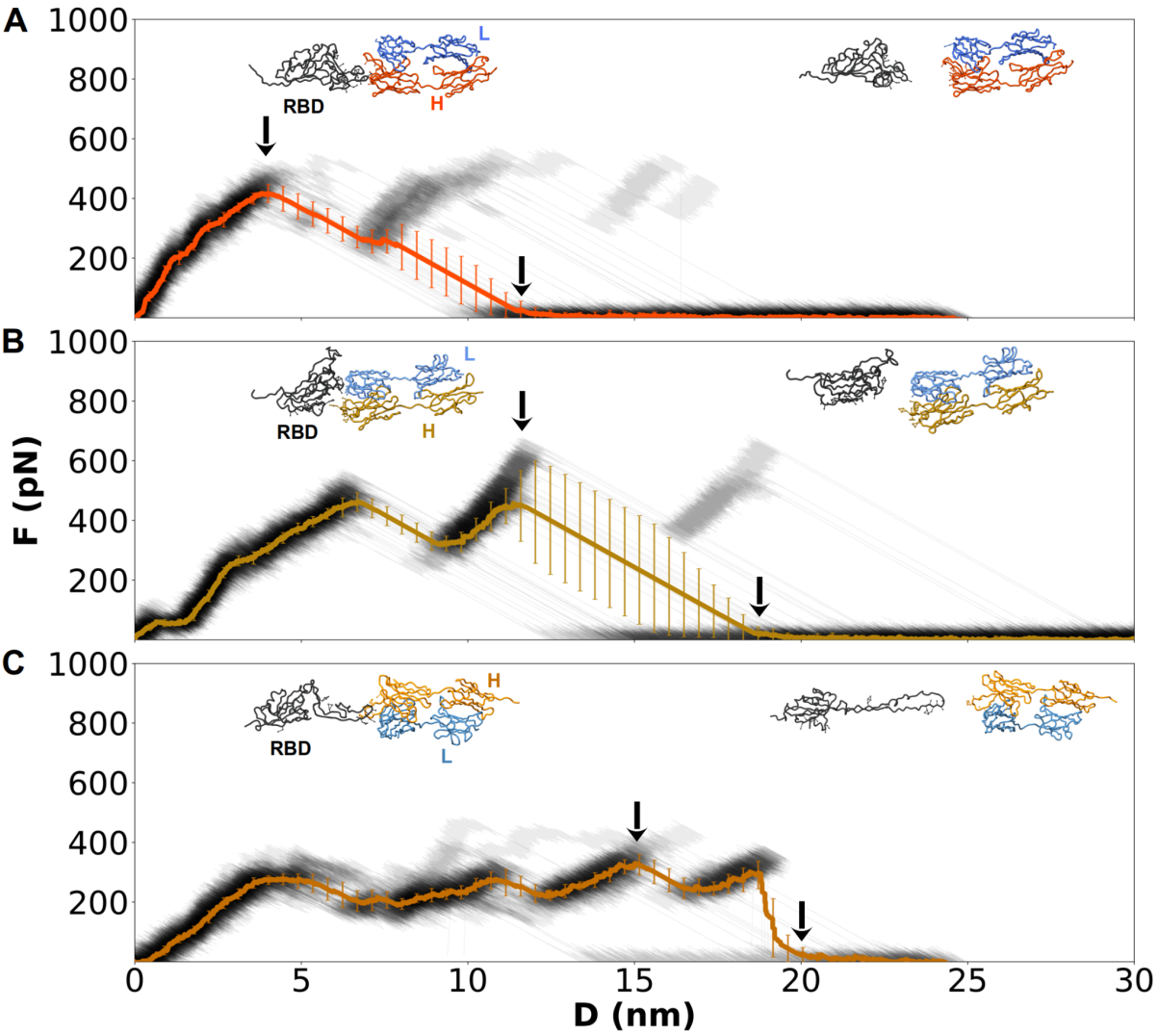

Figure S8. Mechanical response of Ab/RBD BA.4 complexes under constant-velocity pulling from the H chain. Same as Figure S4.

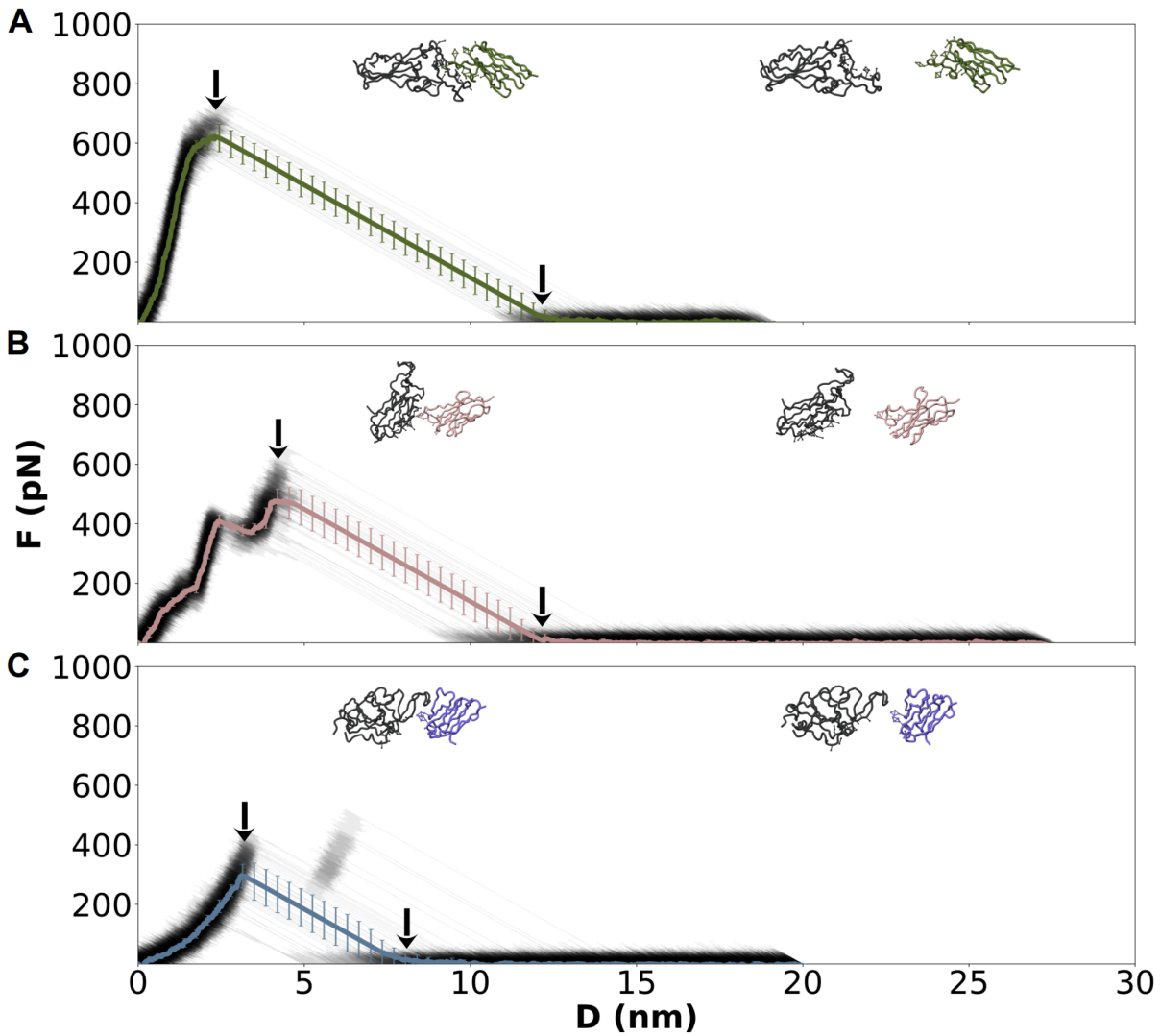

Figure S9. Mechanical response of Nb/RBD BA.4 complexes under constant-velocity pulling. Force–displacement profiles are shown for (A) R14, (B) C1, and (C) n313.1 (gray traces, mean in color). Insets display representative structures at the maximum force (Fmax, left arrow) and after dissociation (right arrow). Error bars denote standard deviations across 50 independent trajectories.

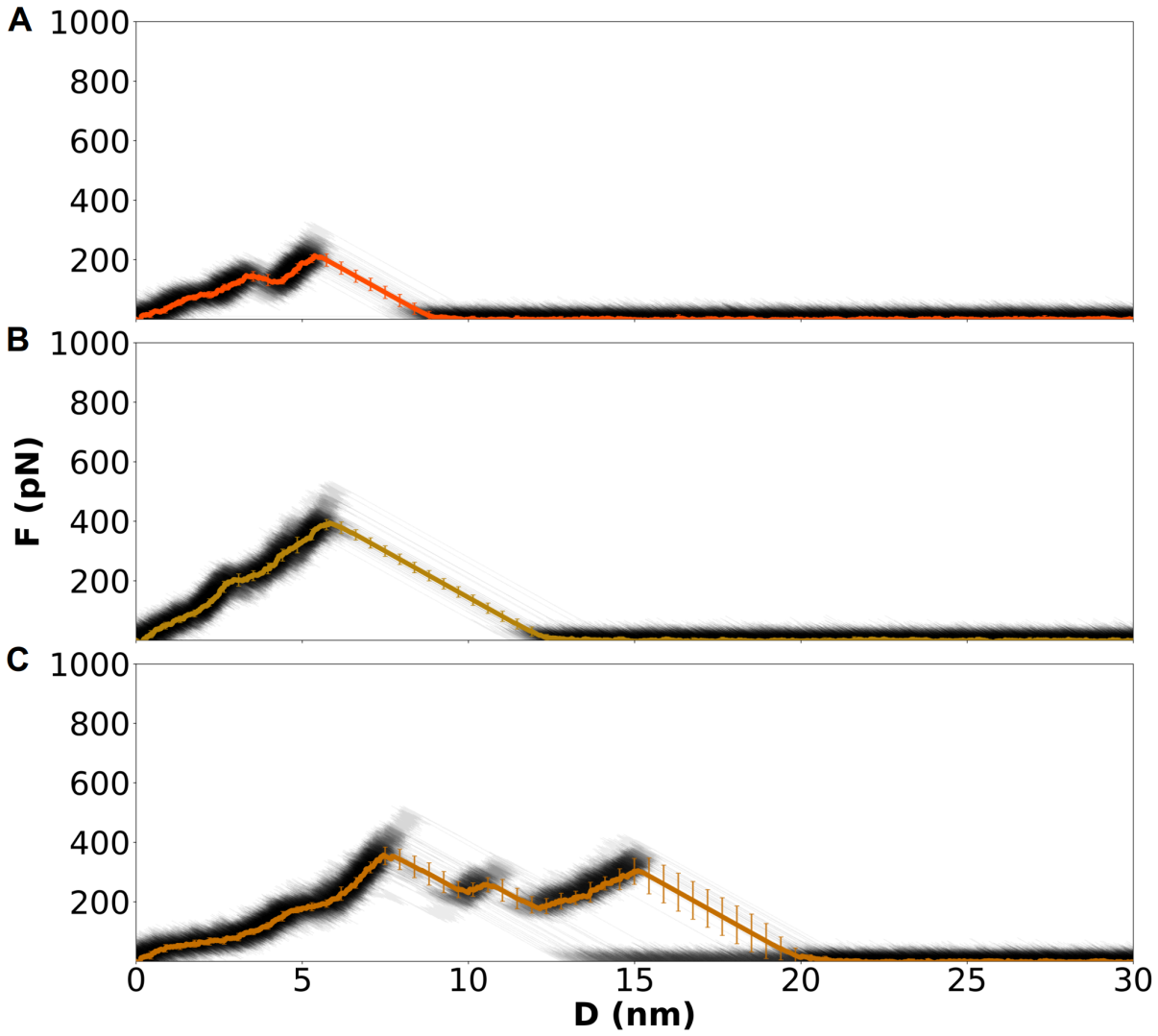

Figure S10. Mechanical response of H chain/RBD WT complexes under constant-velocity pulling from the H chain. Same as Figure S4.

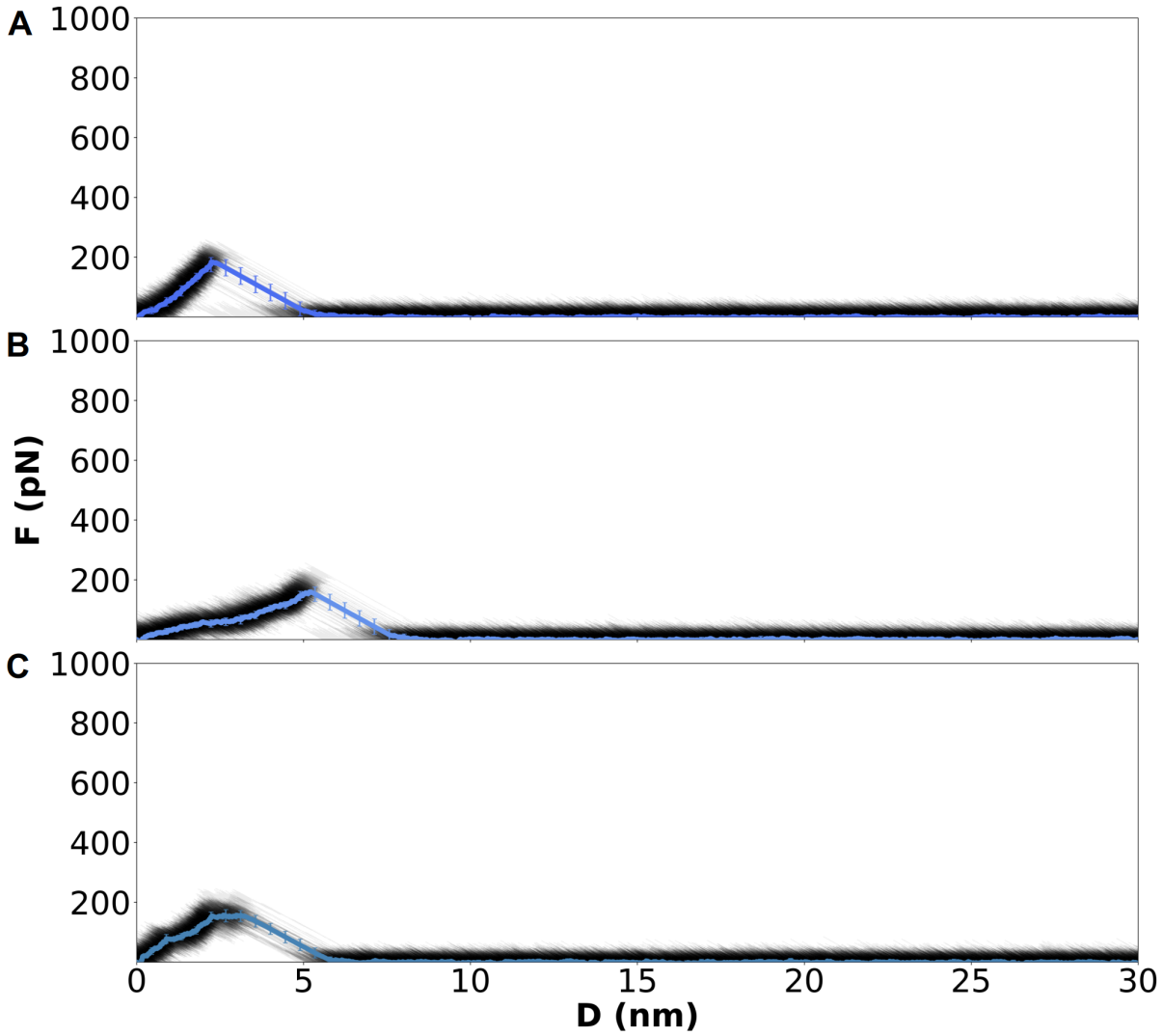

Figure S11. Mechanical response of L chain/RBD WT complexes under constant-velocity pulling from the L chain. Same as Figure S4.

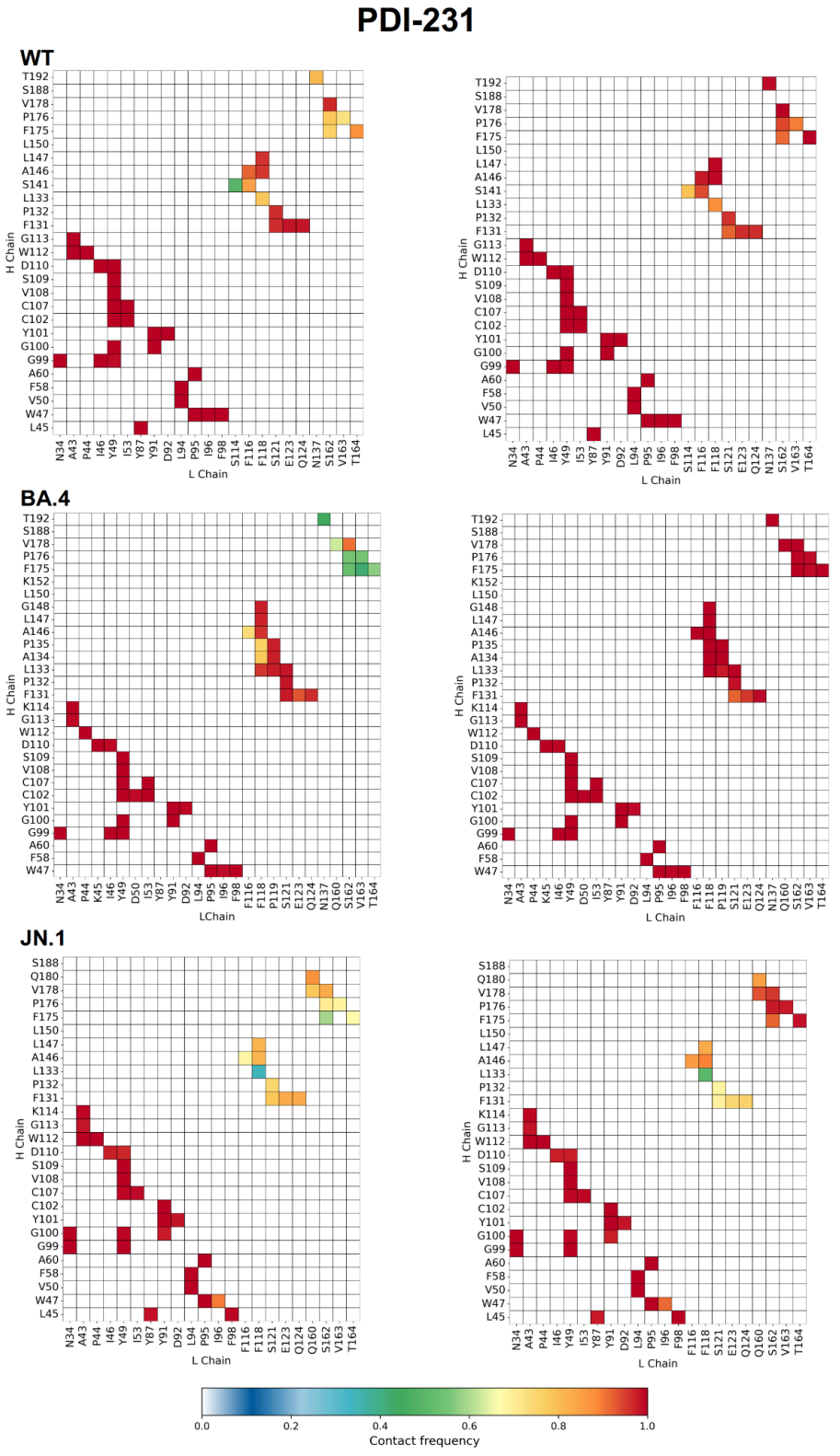

Figure S12. Interchain contact frequency maps for the PDI-231 antibody under directional pulling. Contact maps show the frequency of interchain contacts between the heavy (H) and light (L) chains of the PDI-231 antibody in complex with the SARS-CoV-2 RBD for three viral variants: WT (top), BA.4 (middle), and JN.1 (bottom). The left panels correspond to simulations where pulling was applied to the heavy chain, while the right panels correspond to pulling from the light chain. Contacts were calculated using the extended VdW radii method across 50 steered molecular dynamics trajectories. Color intensity reflects contact frequency.

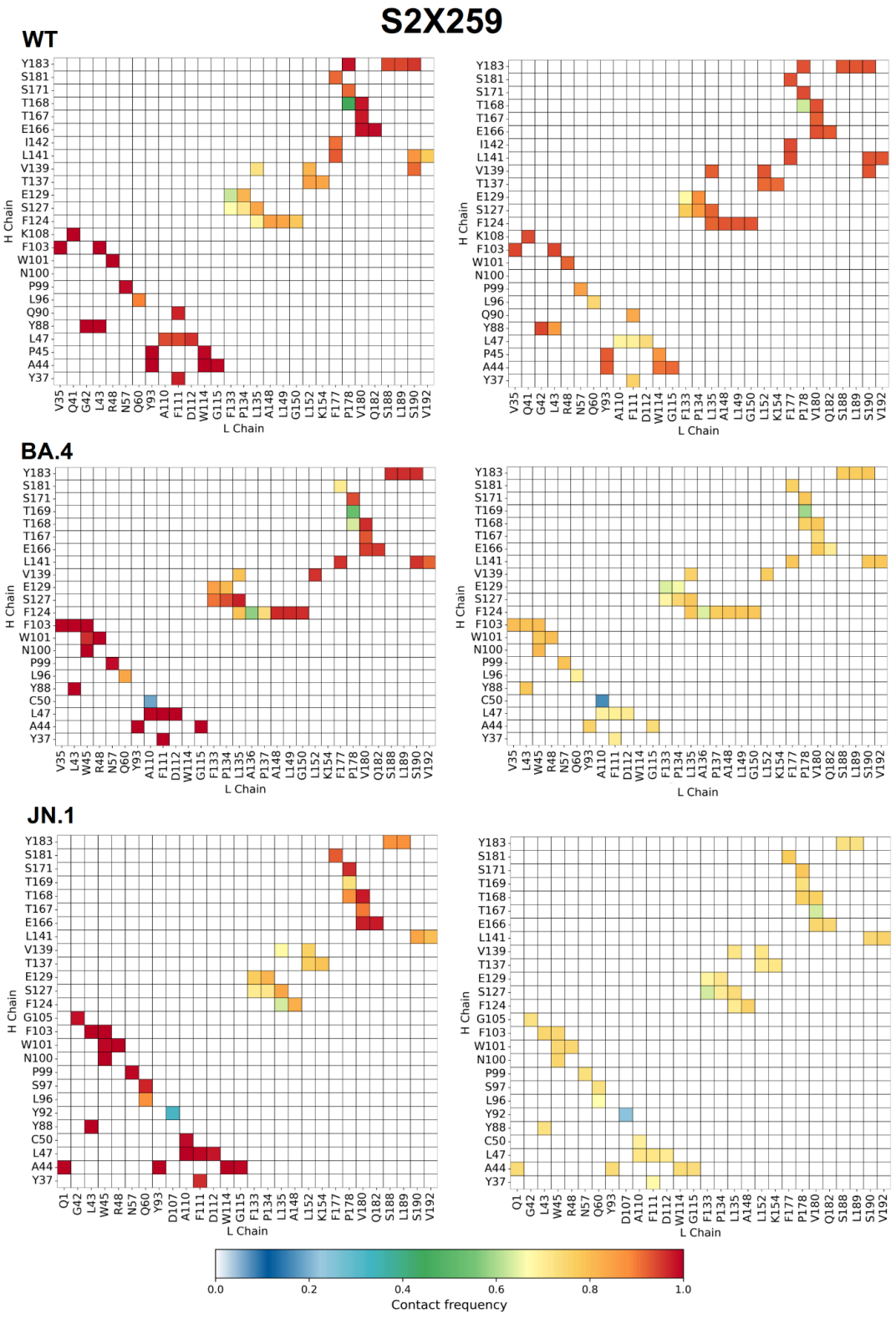

Figure S13. Interchain contact frequency maps for the S2X259 antibody under directional pulling. Contact maps show the frequency of interchain contacts between the heavy (H) and light (L) chains of the S2X259 antibody in complex with the SARS-CoV-2 RBD for three viral variants: WT (top), BA.4 (middle), and JN.1 (bottom). The left panels correspond to simulations where pulling was applied to the heavy chain, while the right panels correspond to pulling from the light chain. Contacts were calculated using the extended VdW radii method across 50 steered molecular dynamics trajectories. Color intensity reflects contact frequency.

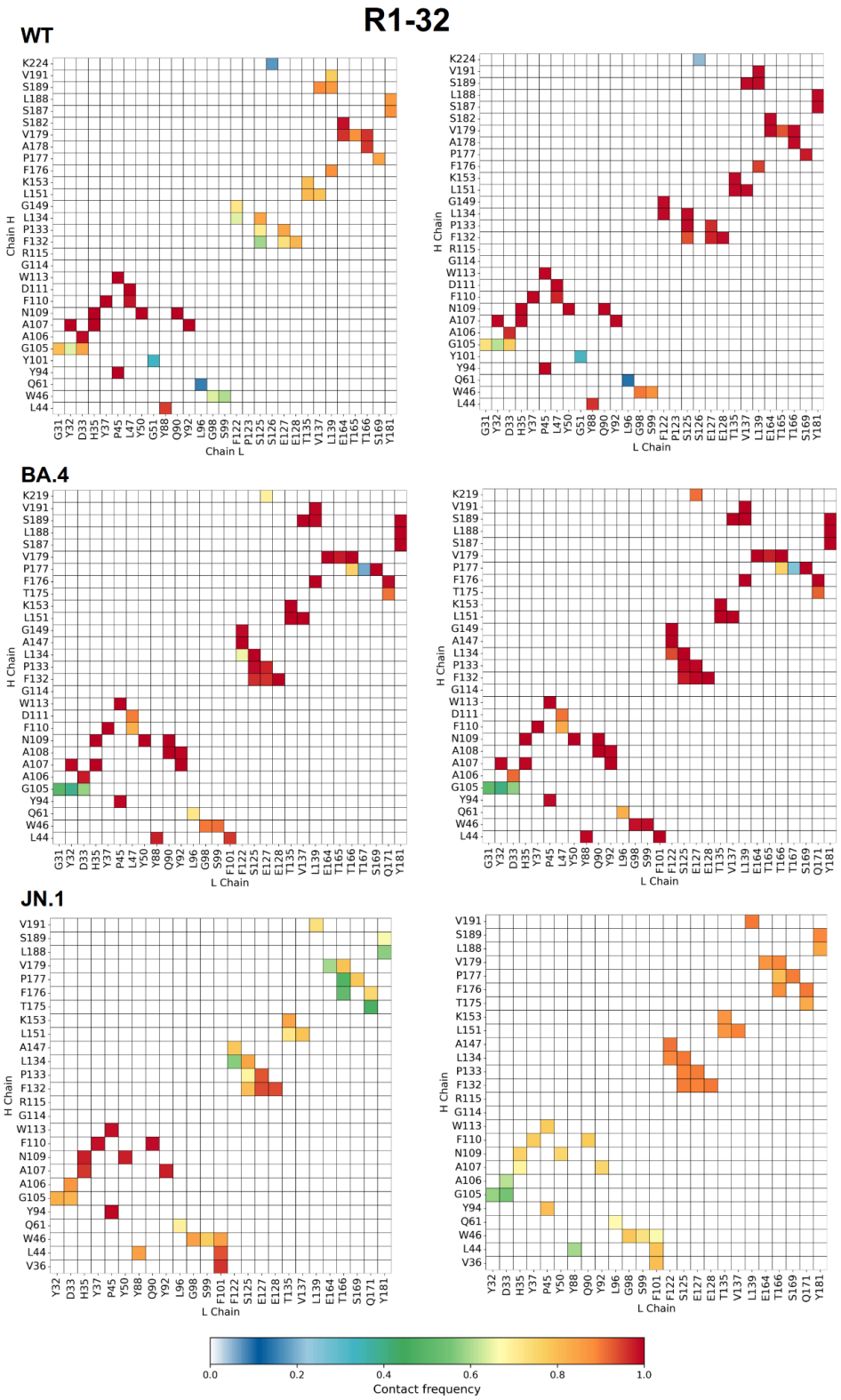

Figure S14. Interchain contact frequency maps for the R1-32 antibody under directional pulling. Contact maps show the frequency of interchain contacts between the heavy (H) and light (L) chains of the R1-32 antibody in complex with the SARS-CoV-2 RBD for three viral variants: WT (top), BA.4 (middle), and JN.1 (bottom). The left panels correspond to simulations where pulling was applied to the heavy chain, while the right panels correspond to pulling from the light chain. Contacts were calculated using the extended VdW radii method across 50 steered molecular dynamics trajectories. Color intensity reflects contact frequency.

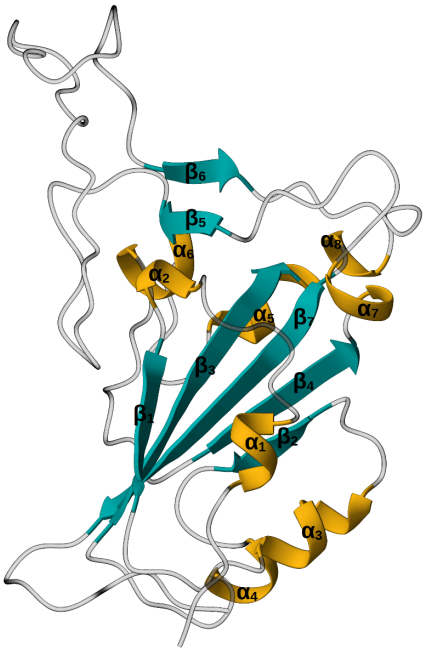

Helix	Residue range	β-strand	Residue range
α_1	338-343	β_1	354-358
α_2	350-352	β_2	376-379
α_3	365-371	β_3	394-403
α_4	384-387	β_4	432-437
α_5	404-409	β_5	452-545
α_6	417-421	β_6	492-494
α_7	439-442	β_7	507-516
α_8	503-505		

Figure S15. Secondary structure elements of the SARS-CoV-2 RBD. The α-helices and β-strands are shown on the RBD cartoon representation, with corresponding residue ranges listed in the table.

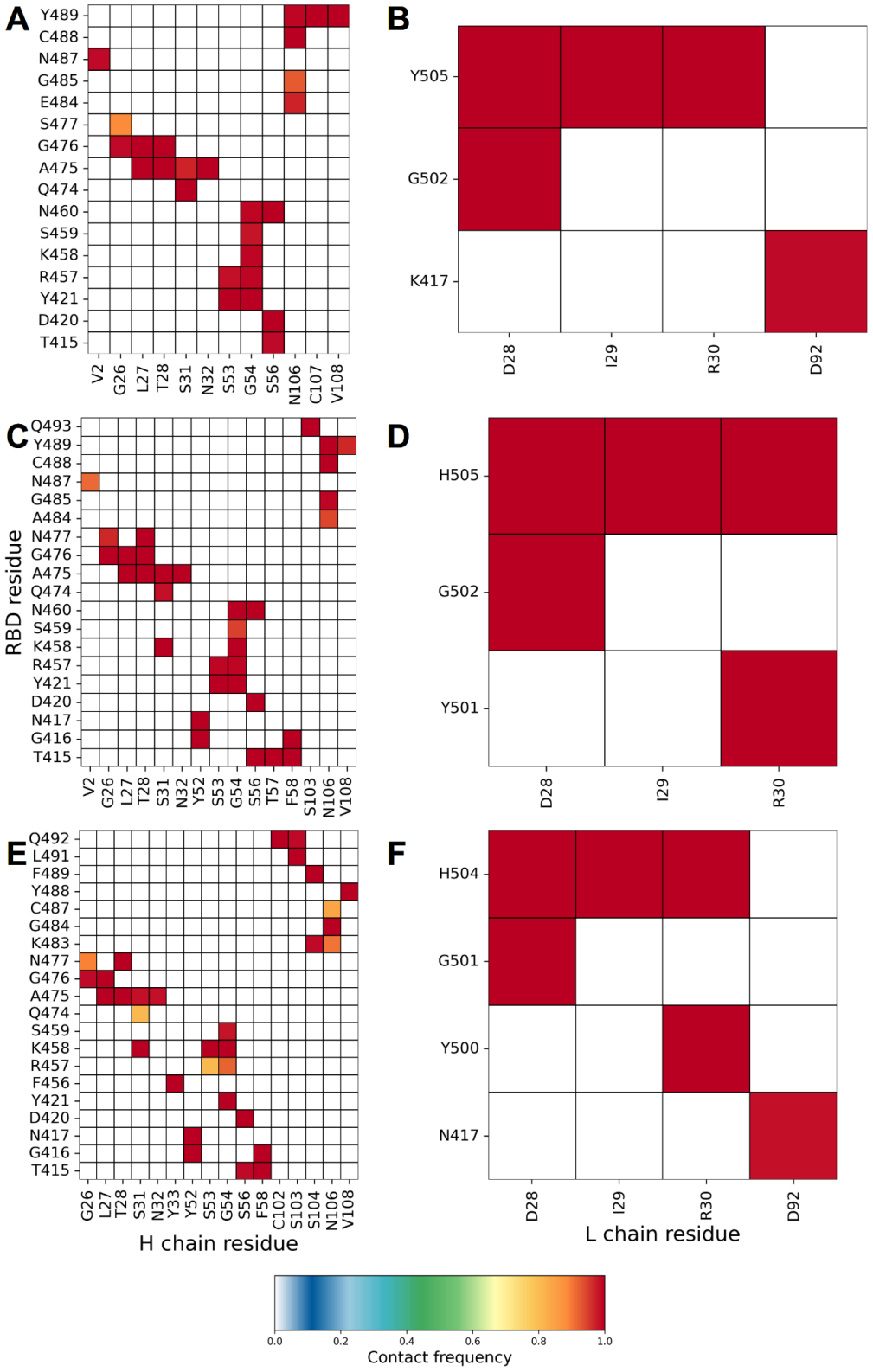

Figure S16. Interchain contact frequency maps for the RBD/PDI-231 complex from equilibrium simulations. Contact maps show the frequency of interchain contacts between the RBD and the H or L chains of the PDI-231 Ab. The left panels correspond to contacts with the H chain, and the right panels to contacts with the L chain. Contacts were computed using the extended van der Waals radii method across five independent CG-MD simulations. Color intensity reflects the frequency of each contact. Panels A and B correspond to the WT complex, panels C and D to the BA.4 complex, and panels E and F to the JN.1 complex.

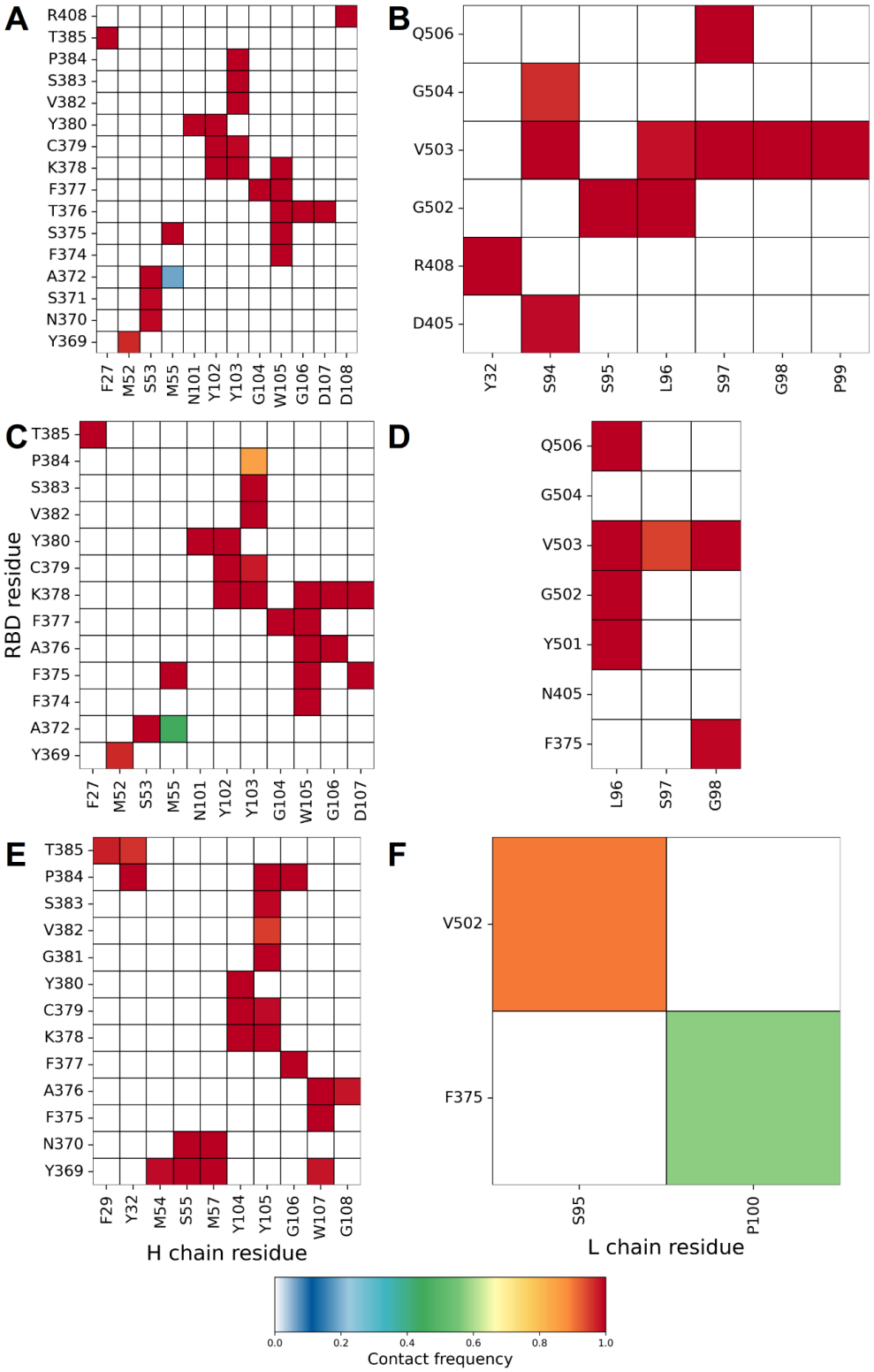

Figure S17. Interchain contact frequency maps for the RBD/S2X259 complex from equilibrium simulations. Same as Figure S13.

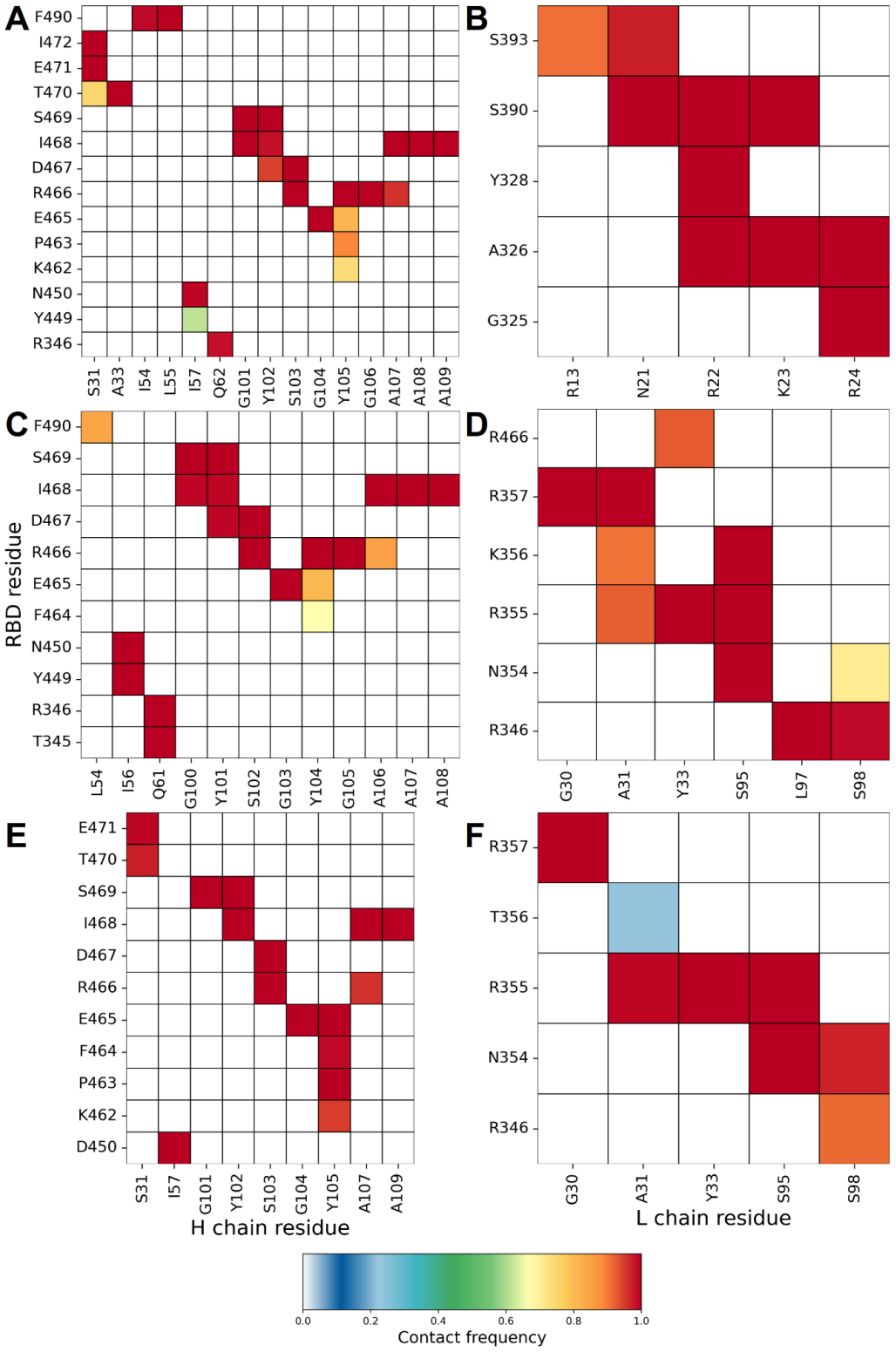

Figure S18. Interchain contact frequency maps for the RBD/R1-32 complex from equilibrium simulations. Same as Figure S13.

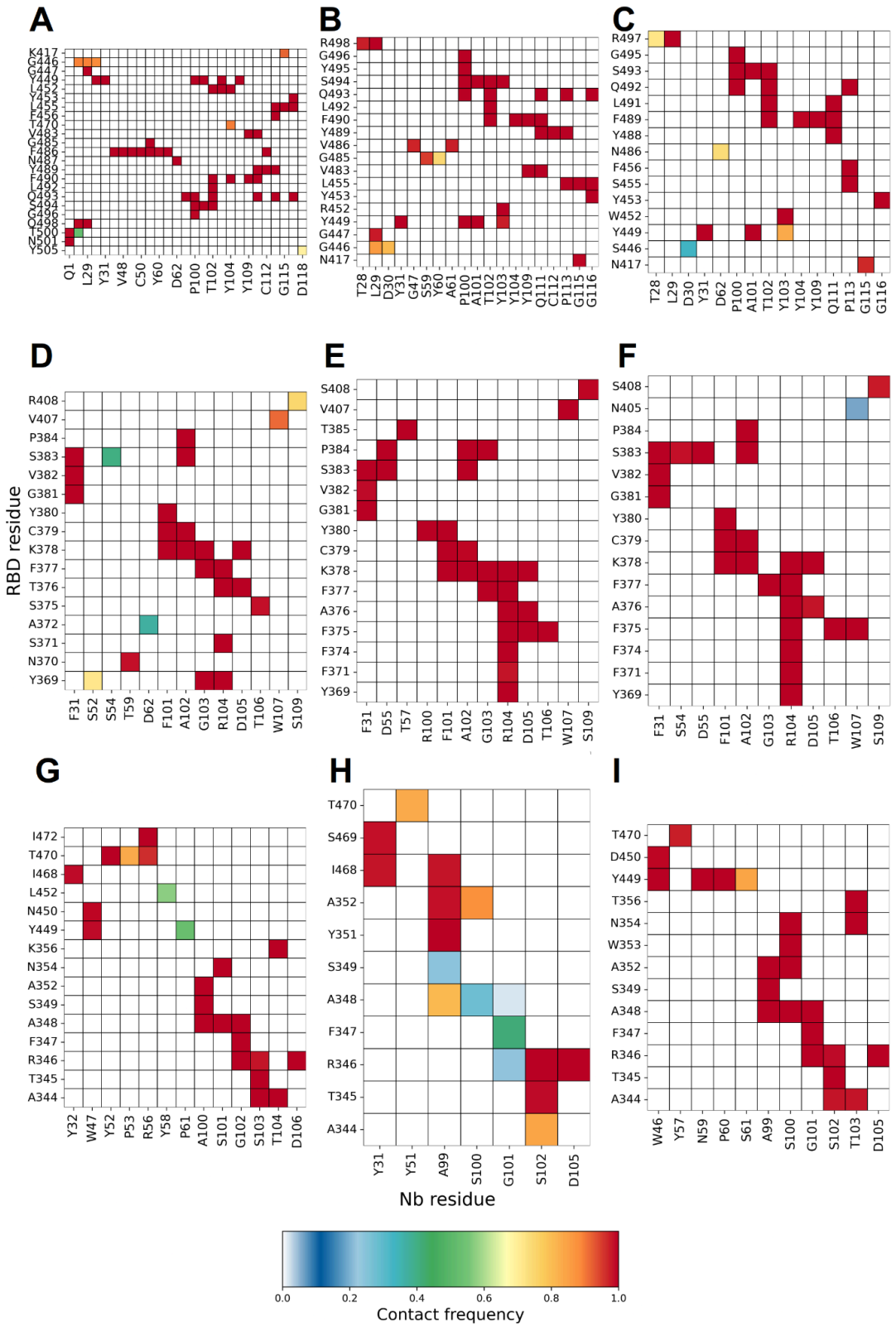

Figure S19. Interchain contact frequency maps for the RBD/Nb complexes from equilibrium simulations. Contact maps show the frequency of interchain contacts between the RBD and nanobodies R14, C1, and n3113.1. Contacts were computed using the extended van der Waals radii method across five independent coarse-grained molecular dynamics simulations. Color intensity reflects the frequency of each contact, from rare (blue) to persistent (red). Panels A, D, and G correspond to the WT complex; panels B, E, and H to the BA.4 complex; and panels C, F, and I to the JN.1 complex. Rows correspond to the different nanobodies: the first row to R14 (A–C), the second row to C1 (D–F), and the third row to n3113.1 (G–I).

Table S1. Structural and binding parameters of the selected nanobodies targeting the SARS-CoV-2 RBD. For each protein case, the name, type, PDB ID, and RBD residues making contacts with the WT are listed. Experimental dissociation constant (KD) parameters considering different variants are reported. Residues in bold are part of the RBM region.

Ab	R14 (PDB ID: 7MZN)			C1 (PDB ID: 7OAP)			n3113.1 (PDB ID: 7VNE)		
Variant	WT	BA.4	JN.1	WT	BA.4	JN.1	WT	BA.4	JN.1
	K417	N417	N417	Y369	*	*	A344	*	*
	G446	*	**S446**	N370	-	-	T345	*	*
	G447	*	**-**	S371	-	-	F347	*	*
	L452	**R452**	**W452**	A372	-	*	A348	*	*
	L455	*	*	S375	-	-	A352	*	*
	F456	**-**	**-**	T376	-	-	R346	*	*
	Y449	*	*	F377	*	*	S349	*	*
	Y453	*	*	C379	*	*	-	**-**	**W353**
	F486	**-**	**N486**	Y380	*	*	**N354**	**-**	*
	F490	*	*	G381	*	*	K356	-	-
	L492	*	*	V382	*	*	**Y449**	-	*
	Q493	*	*	P384	*	*	**N450**	**-**	**-**
	Q498	**R498**	**R498**	-	-	N405	**L452**	**-**	**-**
	Y489	*	*	V407	*	-	**I468**	*	**-**
	G496	*	*	R408	-	-	**T470**	*	**-**
	S494	*	*				**I472**	**-**	**-**
	T500	**-**	**-**						
Kd app. (nM)	ND[a,b*31] 0.02[c*31] 0.03[d*31] 43.3[f*3]			0.615[a*32] 0.725[b*32] 0.648[c*32]			6.4[a**33]		

ND refers to no dissociation.

[a]WT
[b]Alpha
[c]Beta
[d]Gamma
[e]Delta
[f]Omicron BA.4/5

*Surface plasmon resonance (SPR)
**Bio-layer interferometry (BLI)

Table S2. List of protein contacts at the RBD/PDI-231 interface. Protein-protein interactions were calculated using the OV+rCSU contact map protocol over an MD trajectory of 500 ns. Protein contacts with a frequency of 0.7 were considered in the contact map. The total number of protein contacts is given next to the RBD variant name. Residues from RBD are shown in bold. Hydrophobic, hydrophilic, and ionic contacts are highlighted in green, blue, and red, respectively.

Chain	WT (31)	BA.4 (38)	JN.1 (39)
H	**A475**-L27 **A475**-N32 **A475**-S31 **A475**-T28 - **C488**-N106 **D420**-S56 **E484**-N106 - - - - **G476**-G26 **G476**-L27 **G476**-T28 **G485**-N106 **K458**-G54 - - - - - - **N460**-G54 **N460**-S56 - - **N487**-V2 **Q474**-S31 - - **R457**-G54 **R457**-S53 **S459**-G54 **S477**-G26 - **T415**-S56 - **Y421**-G54 **Y421**-S53 **Y489**-C107 **Y489**-N106 **Y489**-V108	**A475**-L27 **A475**-N32 **A475**-S31 **A475**-T28 **A484**-N106 **C488**-N106 **D420**-S56 - - - **G416**-F58 **G416**-Y52 **G476**-G26 **G476**-L27 **G476**-T28 **G485**-N106 **K458**-G54 **K458**-S31 - - - - **N417**-Y52 **N460**-G54 **N460**-S56 **N477**-G26 **N477**-T28 **N487**-V2 **Q474**-S31 - **Q493**-S103 **R457**-G54 **R457**-S53 **S459**-G54 - **T415**-F58 **T415**-S56 **T415**-T57 **Y421**-G54 **Y421**-S53 - **Y489**-N106 **Y489**-V108	**A475**-L27 **A475**-N32 **A475**-S31 **A475**-T28 - **C488**-N106 **D420**-S56 - **F456**-Y33 **F489**-S104 **G416**-F58 **G416**-Y52 **G476**-G26 **G476**-L27 **G476**-T28 **G485**-N106 **K458**-G54 **K458**-S31 **K458**-S53 **K483**-N106 **K483**-S104 **L492**-S103 **N417**-Y52 - - **N477**-G26 **N477**-T28 - **Q474**-S31 **E493**-C102 **E493**-S103 **R457**-G54 **R457**-S53 **S459**-G54 - **T415**-F58 **T415**-S56 - **Y421**-G54 - - - **Y489**-V108
L	**K417**-D92 - **G502**-D28 **Y505**-D28 **Y505**-I29 **Y505**-R30	- **Y501**-R30 **G502**-D28 **H505**-D28 **H505**-I29 **H505**-R30	**N417**-D92 **Y501**-R30 **G502**-D28 **H505**-D28 **H505**-I29 **H505**-R30

Table S3. List of protein contacts at the RBD/S2X259 interface. Protein-protein interactions were calculated using the OV+rCSU contact map protocol over an MD trajectory of 500 ns. Protein contacts with a frequency of 0.7 were considered in the contact map. The total number of protein contacts is given next to the RBD variant name. Residues from the heavy chain are shown in bold. Hydrophobic, hydrophilic, and ionic contacts are highlighted in green, blue, and red, respectively.

Chain	WT (36)	BA.4 (37)	JN.1 (25)
H	**A372**-M55 **A372**-S53 - - **C379**-Y102 **C379**-Y103 **F374**-W105 - **S375**-M55 **S375**-W105 **F377**-G104 **F377**-W105 - - - **K378**-W105 **K378**-Y102 **K378**-Y103 - **N370**-S53 - **P384**-Y103 - **R408**-D108 **S371**-S53 **S383**-Y103 **T376**-D107 **T376**-G106 **T376**-W105 **T385**-F27 - **V382**-Y103 **Y369**-M52 - - - **Y380**-N101 **Y380**-Y102	**A372**-M55 **A372**-S53 **A376**-G106 **A376**-W105 **C379**-Y102 **C379**-Y103 **F374**-W105 **F375**-D107 **F375**-M55 **F375**-W105 **F377**-G104 **F377**-W105 - **K378**-D107 **K378**-G106 **K378**-W105 **K378**-Y102 **K378**-Y103 - - - **P384**-Y103 - - - **S383**-Y103 - - - **T385**-F27 - **V382**-Y103 - - - **Y380**-N101 **Y380**-Y102	- - **A376**-G106 **A376**-W105 **C379**-Y102 **C379**-Y103 - - - **F375**-W105 **F377**-G104 - **G381**-Y103 - - - **K378**-Y102 **K378**-Y103 **N370**-M55 **N370**-S53 **P384**-G104 **P384**-Y103 **P384**-Y30 - - **S383**-Y103 - - - **T385**-F27 **T385**-Y30 **V382**-Y103 **Y369**-M52 **Y369**-M55 **Y369**-S53 **Y369**-W105 - **Y380**-Y102
L	**D405**-S95 - **G502**-L97 - **G502**-S96 - **G504**-S95 - **Q506**-S98 **R408**-Y33 **V503**-G99 **V503**-L97 **V503**-P100 **V503**-S95 **V503**-S98 -	- **F375**-P100 **G502**-L97 **G502**-S95 - **G502**-S98 **G504**-S95 **N405**-Y33 **Q506**-S98 - **V503**-G99 **V503**-L97 **V503**-P100 **V503**-S95 **V503**-S98 **Y501**-S98	- **F375**-P100 - - - - - - - - - - - **V503**-S95 - -

Table S4. List of protein contacts at the RBD/R1-32 interface. Protein-protein interactions were calculated using the OV+rCSU contact map protocol over an MD trajectory of 500 ns. Protein contacts with a frequency of 0.7 were considered in the contact map. The total number of protein contacts is given next to the RBD variant name. Residues from the heavy chain are shown in bold. Hydrophobic, hydrophilic, and ionic contacts are highlighted in green, blue, and red, respectively.

Chain	WT (36)	BA.4 (33)	JN.1 (24)
H	- - - **D467**-Y102 - - **E465**-Y105 **E471**-S31 - - **F490**-I54 **F490**-L55 **E465**-G104 - **I468**-A107 **I468**-A108 **I468**-A109 - **I468**-G101 - **I57**-N450 **K462**-Y105 - **P463**-Y105 - **R346**-Q62 - **R466**-A107 - **R466**-G106 - - - **R466**-Y105 **S103**-D467 **S103**-R466 **I472**-S31 - **S469**-G101 - - **T470**-A33 **T470**-S31 **I468**-Y102 **S469**-**Y102** - **Y449**-I57	- **D467**-S103 **D467**-G101 - **E465**-S103 **E465**-G104 - - **F464**-G104 - **F490**-I54 - - **I468**-G106 **I468**-A107 **I468**-A108 - **I468**-N100 **I468**-G101 - - - **N450**-G56 - **R346**-A61 - **R466**-G106 - **R466**-Y105 - **R466**-Y102 - **R466**-G104 - - - - **S469**-N100 **S469**-G101 - **T345**-A61 - - - - **Y449**-G56 -	**D450**-I57 **D467**-S103 - - - **E465**-G104 **E465**-Y105 **E471**-S31 - **F464**-Y105 - - - - **I468**-A107 - **I468**-A109 - - **I468**-Y102 - **K462**-Y105 - **P463**-Y105 - - - **R466**-A107 - - - **R466**-S103 - - - - - **S469**-G101 **S469**-Y102 - - **T470**-S31 - - - -
L	**A326**-K23 **A326**-R22 **A326**-R24 **G325**-R24 - - - - - - - - - - - - **S390**-K23	- - - - **K356**-A31 **K356**-S95 **N354**-S95 **N354**-S98 **R346**-L97 **R346**-S98 **R355**-A31 **R355**-S95 **R355**-Y33 **R357**-A31 **R357**-G30 **R466**-Y33 -	- - - - - - **N354**-S95 **N354**-S98 - **R346**-S98 **R355**-A31 **R355**-S95 **R355**-Y33 - **R357**-G30 - -

	S390-N21 **S390**-R22 **S393**-N21 **S393**-R13 - **Y328**-R22	- - - - - -	- - - - **T356**-A31 -

Table S5. List of protein contacts at the RBD/R14 interface. Protein-protein interactions were calculated using the OV+rCSU contact map protocol over an MD trajectory of 500 ns. Protein contacts with a frequency of 0.7 were considered in the contact map. The total number of protein contacts is given next to the RBD variant name. Residues from the heavy chain are shown in bold. Hydrophobic, hydrophilic, and ionic contacts are highlighted in green, blue, and red, respectively.

WT (41)	BA.4 (40)	JN.1 (26)
F456-P113	-	**F456**-P113
F486-A61	-	-
F486-C50	-	-
F486-G47	-	-
F486-S49	-	-
F486-S59	-	-
F486-V48	-	-
F486-Y60	-	-
F490-Q111	**F490**-Q111	**F490**-Q111
F490-T102	**F490**-T102	**F490**-T102
F490-Y104	**F490**-Y104	**F490**-Y104
F490-Y109	**F490**-Y109	**F490**-Y109
G446-D30	**G446**-D30	**S446**-D30
G446-L29	**G446**-L29	-
G446-T28	-	-
G447-L29	**G447**-L29	-
-	**G485**-S59	-
-	**G485**-Y60	-
G496-P100	**G496**-P100	**G496**-P100
K417-G115	**N417**-G115	**N417**-G115
L452-Y103	**R452**-Y103	**W452**-Y103
L455-G115	**L455**-G115	-
L455-G116	**L455**-G116	-
L455-P113	**L455**-P113	**S455**-P113
-	-	**L492**-Q111
-	-	**N486**-D62
L492-T102	**L492**-T102	**L492**-T102
Q493-G116	**Q493**-G116	-
Q493-P100	**Q493**-P100	**Q493**-P100
-	**Q493**-P113	**Q493**-P113
-	**Q493**-Q111	-
Q493-T102	**Q493**-T102	**Q493**-T102
Q498-L29	**R498**-L29	**R498**-L29
Q498-T28	**R498**-T28	**R498**-T28
S494-A101	**S494**-A101	**S494**-A101
S494-P100	**S494**-P100	**S494**-P100
S494-T102	**S494**-T102	**S494**-T102
-	**S494**-Y103	-
T500-T28	-	-
-	**V483**-Q111	-
-	**V483**-Y109	-
-	**V486**-A61	-
-	**V486**-G47	-
Y449-A101	**Y449**-A101	**Y449**-A101
Y449-D30	-	-
Y449-P100	**Y449**-P100	-
Y449-Y103	**Y449**-Y103	**Y449**-Y103
Y449-Y31	**Y449**-Y31	**Y449**-Y31
Y453-G116	**Y453**-G116	**Y453**-G116
-	-	
Y489-C112	**Y489**-C112	-
Y489-P113	**Y489**-P113	-
Y489-Q111	**Y489**-Q111	**Y489**-Q111
-	**Y495**-P100	-

Table S6. List of protein contacts at the RBD/C1 interface. Protein-protein interactions were calculated using the OV+rCSU contact map protocol over an MD trajectory of 500 ns. Protein contacts with a frequency of 0.7 were considered in the contact map. The total number of protein contacts is given next to the RBD variant name. Residues from the heavy chain are shown in bold. Hydrophobic, hydrophilic, and ionic contacts are highlighted in green, blue, and red, respectively.

WT (26)	BA.4 (30)	JN.1 (34)
A372-D62	-	-
-	-	**A372**-R104
-	**A376**-D105	**A376**-D105
-	**A376**-R104	**A376**-R104
C379-A102	**C379**-A102	**C379**-A102
C379-F101	**C379**-F101	**C379**-F101
-	-	**C379**-F31
-	**F371**-R104	**F371**-R104
-	**F374**-R104	**F374**-R104
-	**F375**-D105	-
-	**F375**-R104	**F375**-R104
-	**F375**-T106	**F375**-T106
-	-	**F375**-W107
F377-G103	**F377**-G103	**F377**-G103
F377-R104	**F377**-R104	**F377**-R104
G381-F31	**G381**-F31	**G381**-F31
K378-A102	**K378**-A102	**K378**-A102
K378-D105	**K378**-D105	**K378**-D105
K378-F101	**K378**-F101	**K378**-F101
K378-G103	**K378**-G103	-
-	**K378**-R104	**K378**-R104
-	-	**K378**-S110
N370-T59	-	-
-	-	**N405**-W107
P384-A102	**P384**-A102	**P384**-A102
-	**P384**-D55	-
-	**P384**-G103	-
R408-S109	-	-
S371-R104	-	-
S375-T106	-	-
S383-A102	**S383**-A102	**S383**-A102
-	**S383**-D55	**S383**-D55
S383-F31	**S383**-F31	**S383**-F31
S383-S54	-	**S383**-S54
-	**S408**-S109	**S408**-S109
T376-D105	-	-
T376-R104	-	-
-	-	**T385**-D55
-	**T385**-T57	**T385**-T57
V382-F31	**V382**-F31	**V382**-F31
V407-W107	**V407**-W107	-
Y369-G103	-	**Y369**-G103
Y369-R104	**Y369**-R104	**Y369**-R104
Y369-S52	-	-
-	-	**Y369**-T57
Y380-F101	**Y380**-F101	**Y380**-F101
-	-	**Y380**-F31
-	**Y380**-R100	-

Table S7. List of protein contacts at the RBD/n3113.1 interface. Protein-protein interactions were calculated using the OV+rCSU contact map protocol over an MD trajectory of 500 ns. Protein contacts with a frequency of 0.7 were considered in the contact map. The total number of protein contacts is given next to the RBD variant name. Residues from the heavy chain are shown in bold. Hydrophobic, hydrophilic, and ionic contacts are highlighted in green, blue, and red, respectively.

n3113.1 (PDB ID: 7VNE)		
WT (23)	BA.4 (17)	JN.1 (23)
A344-S103	**A344**-S103	**A344**-S1023
A344-T104	-	**A344**-T104
A348-A100	**A348**-A100	**A348**-A100
A348-G102	**A348**-G102	**A348**-G102
A348-S101	**A348**-S101	**A348**-S101
A352-A100	**A352**-A100	**A352**-A100
-	**A352**-S101	**A352**-S101
-	-	**D450**-W47
F347-G102	**F347**-G102	**F347**-G102
-	-	-
-	**I468**-A100	-
I468-Y32	**I468**-Y32	-
I472-R56	-	-
K356-T104	-	-
L452-Y58	-	-
N354-S101	-	**N354**-S101
N450-W47	-	-
-	-	**N354**-T104
R346-D106	**R346**-D106	**R346**-D106
R346-G102	**R346**-G102	**R346**-G102
R346-S103	**R346**-S103	**R346**-S103
S349-A100	**S349**-A100	**S349**-A100
-	**S469**-Y32	-
T345-S103	**T345**-S103	**T345**-S103
T470-P53	-	-
T470-R56	-	-
-	-	**T356**-T104
T470-Y52	**T470**-Y52	-
-	-	-
-	**Y351**-A100	-
-		**T470**-Y58
-	-	**W353**-S101
-	-	**Y449**-N60
Y449-P61	-	**Y449**-P61
-	-	**Y449**-S62
Y449-W47	-	**Y449**-W47

Table S8. Interchain contacts at the PDI-231 Ab interface. Contacts were identified using the OV+rCSU contact map protocol applied to a 500 ns molecular dynamics trajectory. Only interactions with a frequency of 0.7 or higher were included. Each contact is denoted as a residue pair, where the first residue belongs to the heavy chain and the second to the light chain. The total number of inter-chain contacts is reported for each SARS-CoV-2 RBD variant. Hydrophobic, hydrophilic, and ionic contacts are highlighted in green, blue, and red, respectively.

WT (49)	BA.4 (55)	JN.1 (45)
-	A134-F118	-
-	A134-P119	-
A146-F116	A146-F116	A146-F116
A146-F118	A146-F118	A146-F118
A60-P95	A60-P95	A60-P95
C102-D50	C102-D50	C102-D50
C102-I53	C102-I53	-
C102-Y49	C102-Y49	-
-	-	C102-Y91
C107-I53	C107-I53	C107-I53
C107-Y49	C107-Y49	C107-Y49
D110-I46	D110-I46	D110-I46
D110-K45	D110-K45	-
D110-Y49	-	D110-Y49
F131-E123	F131-E123	F131-E123
F131-Q124	F131-Q124	F131-Q124
F131-S121	F131-S121	F131-S121
F175-S162	F175-S162	F175-S162
F175-T164	F175-T164	F175-T164
-	F175-V163	-
F58-L94	F58-L94	F58-L94
-	-	G100-N34
G100-Y49	G100-Y49	G100-Y49
G100-Y91	G100-Y91	G100-Y91
G113-A43	G113-A43	G113-A43
-	G148-F118	-
G99-I46	G99-I46	-
G99-N34	G99-N34	G99-N34
G99-Y49	G99-Y49	G99-Y49
K114-A43	K114-A43	K114-A43
-	K152-S131	-
L133-F118	L133-F118	L133-F118
-	L133-P119	-
-	L133-S121	-
L147-F118	L147-F118	L147-F118
L150-S131	L150-S131	L150-S131
-	L150-V133	-
-	L45-F98	L45-F98
L45-Y87	L45-Y87	L45-Y87
P132-S121	P132-S121	P132-S121
-	P135-F118	-
-	P135-P119	-
P176-S162	P176-S162	P176-S162
P176-V163	P176-V163	P176-V163
-	-	Q180-Q160
S109-Y49	S109-Y49	S109-Y49
S141-F116	-	-
S141-S114	-	-
S188-S176	S188-S176	S188-S176
T192-N137	T192-N137	-
V108-Y49	V108-Y49	V108-Y49
-	V178-Q160	V178-Q160
V178-S162	V178-S162	V178-S162
V50-L94	-	V50-L94
W112-A43	-	W112-A43
W112-K45	-	-
W112-P44	W112-P44	W112-P44
W47-F98	W47-F98	-
W47-I96	W47-I96	W47-I96
W47-P95	W47-P95	W47-P95

Y101-D92 Y101-Y91 Y94-A43 Y94-P44	Y101-D92 Y101-Y91 Y94-A43 Y94-P44	Y101-D92 Y101-Y91 Y94-A43 Y94-P44

Table S9. Interchain contacts at the S2X259 antibody interface. Contacts were identified using the OV+rCSU contact map protocol applied to a 500 ns molecular dynamics trajectory. Only interactions with a frequency of 0.7 or higher were included. Each contact is denoted as a residue pair, where the first residue belongs to the heavy chain and the second to the light chain. The total number of inter-chain contacts is reported for each SARS-CoV-2 RBD variant. Hydrophobic, hydrophilic, and ionic contacts are highlighted in green, blue, and red, respectively.

WT (46)	BA.4 (49)	JN.1 (46)
-	A110-C50	A110-C50
A110-L47	A110-L47	A110-L47
-	A136-F124	-
A148-F124	A148-F124	A148-F124
-	-	D107-Y92
D112-L47	D112-L47	D112-L47
-	E44-F103	-
F111-L47	F111-L47	F111-L47
F111-Q90	-	-
F111-Y37	F111-Y37	F111-Y37
F133-E129	F133-E129	F133-E129
F133-S127	F133-S127	F133-S127
F177-I142	-	-
F177-L141	F177-L141	-
F177-S181	F177-S181	F177-S181
G115-A44	G115-A44	G115-A44
G150-F124	G150-F124	-
G42-G105	-	G42-G105
K154-T137	K154-T137	K154-T137
L135-F124	L135-F124	L135-F124
L135-S127	L135-S127	L135-S127
L135-V139	L135-V139	L135-V139
L149-F124	L149-F124	-
L152-T137	L152-T137	L152-T137
L152-V139	L152-V139	L152-V139
L189-Y183	L189-Y183	L189-Y183
L43-F103	L43-F103	L43-F103
L43-Y88	L43-Y88	L43-Y88
N57-P99	N57-P99	N57-P99
P134-E129	P134-E129	P134-E129
P134-S127	P134-S127	P134-S127
P137-F124	P137-F124	-
P178-S171	P178-S171	P178-S171
P178-T168	P178-T168	P178-T168
-	P178-T169	P178-T169
P178-Y183	-	-
-	-	Q1-A44
Q182-E166	Q182-E166	Q182-E166
Q41-K108	-	-
Q60-L96	Q60-L96	Q60-L96
-	-	Q60-S97
R48-W101	R48-W101	R48-W101
-	S183-E166	S183-E166
S188-Y183	S188-Y183	S188-Y183
S190-T141	S190-T141	S190-T141
S190-V139	-	-
S190-Y183	S190-Y183	-
V180-E166	V180-E166	V180-E166
V180-T167	V180-T167	V180-T167
V180-T168	V180-T168	V180-T168
V192-L141	V192-L141	V192-L141
V35-F103	V35-F103	-
W114-A44	-	W114-A44
W114-P45	W114-P45	W114-P45
W45-F103	W45-F103	W45-F103
W45-N100	W45-N100	W45-N100
W45-W101	W45-W101	W45-W101
Y93-A44	Y93-A44	Y93-A44
Y93-P45	Y93-P45	Y93-P45

Table S10. Interchain contacts at the R1-32 antibody interface. Contacts were identified using the OV+rCSU contact map protocol applied to a 500 ns molecular dynamics trajectory. Only interactions with a frequency of 0.7 or higher were included. Each contact is denoted as a residue pair, where the first residue belongs to the heavy chain and the second to the light chain. The total number of inter-chain contacts is reported for each SARS-CoV-2 RBD variant. Hydrophobic, hydrophilic, and ionic contacts are highlighted in green, blue, and red, respectively.

WT (52)	BA.4 (54)	JN.1 (45)
A106-D33	A106-D33	A106-D33
A107-H35	A107-H35	A107-H35
A107-Y32	A107-Y32	-
A107-Y92	A107-Y92	A107-Y92
-	A108-Q90	-
-	A108-Y92	-
-	A135-F122	A135-F122
A135-P123	-	-
-	A147-F122	A147-F122
A178-T166	-	-
D111-L47	D111-L47	-
F110-L47	F110-L47	-
-	-	F110-Q90
F110-Y37	F110-Y37	F110-Y37
F132-E127	F132-E127	F132-E127
F132-E128	F132-E128	F132-E128
F132-S125	F132-S125	F132-S125
F176-L139	F176-L139	-
-	F176-Q171	F176-Q171
-	-	F176-T166
G105-D33	G105-D33	G105-D33
G105-G31	G105-G31	-
G105-Y32	G105-Y32	G105-Y32
G114-A44	G114-A44	G114-A44
G149-F122	G149-F122	-
K153-T135	K153-T135	K153-T135
-	K219-E127	-
K224-S126	-	-
L134-F122	L134-F122	L134-F122
L134-S125	L134-S125	L134-S125
L151-T135	L151-T135	L151-T135
L151-V137	L151-V137	L151-V137
L188-Y181	L188-Y181	L188-Y181
L44-F101	L44-F101	L44-F101
L44-Y88	L44-Y88	L44-Y88
N109-H35	N109-H35	N109-H35
N109-Q90	N109-Q90	-
N109-Y50	N109-Y50	N109-Y50
N99-Y50	-	-
P133-E127	P133-E127	P133-E127
P133-S125	P133-S125	P133-S125
P177-S169	P177-S169	P177-S169
-	P177-T166	P177-T166
-	P177-T167	-
Q181-E164	Q181-E164	Q181-E164
Q61-L96	Q61-L96	Q61-L96
R115-A44	-	R115-A44
S182-E164	-	-
S187-Y181	S187-Y181	-
S189-L139	S189-L139	-
S189-V137	S189-V137	-
-	S189-Y181	S189-Y181
-	T175-Q171	T175-Q171
V179-E164	V179-E164	V179-E164
V179-T165	V179-T165	-
V179-T166	V179-T166	V179-T166
V191-L139	V191-L139	V191-L139
-	-	V36-F101
W113-P45	W113-P45	W113-P45

W46-F101 W46-G98 W46-S99 - Y101-G51 Y94-A44 Y94-P45	- W46-G98 W46-S99 - - Y94-A44 Y94-P45	W46-F101 W46-G98 W46-S99 Y101-D33 - Y94-A44 Y94-P45

Table S11. Average Fmax obtained from CG-SMD pulling simulations of Ab and Nb complexes with the RBD in WT, BA.4, and JN.1 variants. Values are reported as mean ± standard deviation across 50 trajectories. For Ab/RBD WT complexes, results are shown for the complete complex (both chains) and for single-chain systems (only H or only L), highlighting the cooperative contribution of dual-chain architecture to mechanical stability.

	Average F_{max} (pN)		
System	**WT**	**BA.4**	**JN.1**
PDI-231 (both)	365.3 ± 30.1	472.1 ± 45.3	388.3 ± 42.5
PDI-231 (only H)	250.2 ± 25.4	-	-
PDI-231 (only L)	208.3 ± 31.9	-	-
S2X259 (both)	549.5 ± 54.2	472.1 ± 45.3	513.2 ± 61.0
S2X259 (only H)	427.6 ± 50.7	-	-
S2X259 (only L)	196.4 ± 24.8	-	-
R1-32 (both)	407.9 ± 45.2	374.9 ± 40.4	390.4 ± 70.4
R1-32 (only H)	405.2 ± 15.3	-	-
R1-32 (only L)	199.7 ± 20.0	-	-
R14	595.9 ± 55.6	648.6 ± 43.7	346.2 ± 34.4
C1	479.5 ± 88.2	513.2 ± 61.0	603.0 ± 55.2
n3113.1	430.5 ± 59.9	336.2 ± 74.6	520.7 ± 68.2